Rev. Téc. Ing., Univ. Zulia
Vol. 6, Edición Especial, 1983

TORQUEWHIRL-A THEORY TO EXPLAIN NONSYNCHRONOUS WHIRLING FAILURES OF ROTORS WITH HIGH LOAD TORQUE

John M. Vance
Professor
Mechanical Engineering
Texas A&M University
College Station, Texas 77843

(Al Libertador Simón Bolívar,
en el bicentenario de su nacimiento)

ABSTRACT

Numerous unexplained failures of rotating machinery by nonsynchronous shaft whirling point to a possible driving mechanism or source of energy not identified by previously existing theory. A majority of these failures have been in machines characterized by overhung disks (or disks located close to one end of a bearing span) and/or high horse power and load torque.

This paper gives exact solutions to the nonlinear differential equations of motion for a rotor having both of these characteristics, and shows that high ratios of driving torque to damping can produce nonsynchronous whirling with destructively large amplitudes. Solutions are given for two cases: (1) viscous load torque and damping, and (2) load torque and damping proportional to the second power of velocity (aerodynamic case).

Linearized coefficients for stability analyses are derived for a special case.

Criteria are given for avoiding the torquewhirl condition.

RESUMEN

Numerosas fallas aún no explicadas en máquinas rotatorias por "whirling" asincronico de ejes sugieren un posible mecanismo o fuente de energía no identificada por las teoricas actuales. Una gran mayoria de estas fallas han sido en máquinas caracterizadas por discos ubicados cerca de uno de los cojinetes y/o alta potencia y momento torsor.

En este trabajo se presentan soluciones analíticas de las ecuaciones diferenciales no lineales de movimiento para un rotor con ambas características, y se demuestra que una relación entre el momento torsor y el amortiguamiento grande puede producir "whirling" asincronico con grandes amplitudes. Las soluciones se dan para dos casos (1) carga de torsión y amortiguamiento viscoso y (2) carga de torsión y amortiguamiento proporcional a la segunda potencia de la velocidad (caso aerodinámico).

Se derivan, para un caso especial, coeficientes linearizados para los análisis de estabilidad. Además se presentan criterios para evitar condiciones de "torquewhirl".

INTRODUCTION

There is a history of nonsynchronous whirling problems in rotating machinery which can be related to the load torque on fluid impellers or bladed disks. Typically, the rotor configuration involves overhung (cantilevered) disks, or disks located asymmetrically (near one end) of a bearing span. Often, the dependence on load torque would have to be inferred, as for example, where the whirling seems to be dependent on the density of the working fluid [1][1], or on the load horse-power [2,3].

This paper presents a theory which shows that, if the load torque on a coning disk tends to remain aligned with the disk axis, as in a fluid impeller, nonsynchronous whirling can be produced as a dynamic equilibrium motion, with an amplitude which depends on the ratio of torque to damping.

A review of the rotor dynamics literature shows that it has been common practice to eliminate the driving torque and load torque from the equations of motion in order to simplify the analysis of lateral whirling. Two examples are references 4 and 5. This procedure is mathematically correct, but obviously is not suited to a study of the effect of torque on the motion. For rotors with disks which remain aligned with the bearing axis (i.e. centered on the bearing span, as in reference 5), the main effect of constant load torque is simply to lower the critical speed [6]. However, if the disk is overhung, or located near one end of a bearing span so that it can execute a coning motion, Bousso [7] has shown that the disk load torque may not be in equilibrium with the driving torque. Bousso's analysis is incomplete, as he does not show necessary or sufficient conditions for torque-driven whirl to ocurr, but his vector diagrams show revealingly how a component of the driving torque can act on the precession coordinate of a coning disk to feed energy into the whirling motion.

This latter effect, which does not requiere a time-varying torque, should be properly differentiated from the effects of torque on rotor response described in reference [6] by Eshleman and Eubanks. Their experimental study showed that a pulsating torque of small magnitude superimposed on a constant torque produces unstable whirling over a range of speed which becomes wider with increasing torque. The instability disappears when the pulsat-

[1] Numbers in brackets refer to the list entitled References.

ing component of the torque is removed. Coning motion of the disk apparently was not a significant factor in their model.

The analysis presented below shows that constant torque at constant speed can produce nonsynchronous whirling if the disk motion is conical.

THE ROTOR MODEL

Figure 1 shows the model analyzed. This is the simplest possible model which has all of the characteristics necessary to produce the phenomenon under study. These are:

(1) The load torque $\vec{T}_L$ on the disk remains parallel to the disk axis (z). The vanes in the disk in Fig. 1 are suggestive of the type of machine which would approximate this condition. Impellers and bladed disks are normally designed to maximize the torque (associated with useful work) produced by rotation about the disk axis.

(2) The driving or shaft torque $\vec{T}_S$ is aligned with the bearing axis (Z). In a machine this torque is often transmitted to the rotor through a shaft coupling, which is idealized by the joint at O'.

(3) The whirling mode is conical, with an amplitude described by the angle θ.

(4) Whirling of the disk produces a damping (drag) force on the disk, not shown in the figure. This force $\vec{F}_d$ is tangential to the path of the disk center C, and produces the moments required for dynamic equilibrium under steady-state conditions. Note that $\vec{T}_L$ and $\vec{T}_S$ cannot be in equilibrium without $\vec{F}_d$, unless $\theta = 0$ [7].

To avoid unnecessary analytical complexity, the shaft is assumed rigid (except at O') and all of the mass (M) of the rotor is concentrated in the disk. Unbalance is not included in the present analysis, so e = 0.

The mass properties of the rotor are completely represented by M and by mass moments of inertia $I_{x'} = I_{y'}$ and I_z about principal axes x' y' z through the point O'. These axes, and parallel axes x y z through C, are fixed in and rotate with the rotor. Axes X' Y' Z, and parallel axes X Y Z, are fixed in space with Z along the bearing axis.

The rotor stiffness K_θ is assumed to produce a restoring moment proportional to θ, $M_n = -K_\theta\theta$. This could be due to shaft bending stiffness or coupling stiffness at O', or a flexible bearing support outboard of the disk. This stiffness is represented graphically in the figure by a spring at OC. In addition, the rotor is assumed to be vertical, so that gravity produces an additional restoring moment[2] of magnitude Mg sinθ.

2. In most real machines, this term is insignificant when compared to the restoring moment of the shaft or coupling.

Both viscous and aerodynamic models are used to describe the velocity dependence of the load torque and the damping force. The corresponding expressions for generalized forces are given in a section below.

The motion and instantaneous position of the rotor can be completely described by specifying the three coordinates z, θ, and ψ as functions of time. These may be recognized as the three Euler angles defined by Goldstein [8]. For conical motion, with circular orbits of the disk center C, the precession or whirling velocity is $\frac{d\phi}{dt} = \dot{\phi}$, the amplitude of whirling is θ = constant, and the shaft speed $\omega_S = \omega_Z = \dot{\phi} + \dot{\psi}$. The rotational speed of the disk is $\omega_Z = \dot{\phi}\cos\theta + \dot{\psi}$. The inequality of the latter two angular velocities is central to an understanding of how torquewhirl is produced. Note that the rotational velocity ω_Z of the disk becomes zero when $\theta = 90°$, $\dot{\psi} = 0$, $\omega_S = \dot{\phi}$. Under this (improbable) condition, all of the shaft work would have to be dissipated by damping, and $\vec{T}_L = 0$.

EQUATIONS OF MOTION

The Lagrangian of the rotor described in the preceding section is derived in Appendix A. Using the methods of references 9 and 10, the six first-order equations of motion are obtained as:

$$\dot{\theta} = \frac{1}{I_{x'}} p_\theta, \tag{1}$$

$$\dot{\phi} = \frac{1}{I_{x'}\sin^2\theta} p_\phi - \frac{\cos\theta}{I_{x'}\sin^2\theta} p_\psi, \tag{2}$$

$$\dot{\psi} = -\frac{\cos\theta}{I_{x'}\sin^2\theta} p_\phi + \left[\frac{1}{I_z} + \frac{\cot^2\theta}{I_{x'}}\right] p_\psi, \tag{3}$$

$$\dot{p}_\theta = \frac{\cos\theta}{I_{x'}\sin^3\theta} p_\phi^2 - \left[\frac{1}{I_{x'}\sin\theta} + \frac{2\cos^2\theta}{I_{x'}\sin^3\theta}\right] p_\phi p_\psi + \left[\frac{\cot\theta}{I_{x'}} + \frac{\cot^3\theta}{I_{x'}}\right] p_\psi^2 - K_\theta\theta - Mg\ell\sin\theta + Q_\theta, \tag{4}$$

$$\dot{p}_\phi = Q_\phi, \tag{5}$$

$$\dot{p}_\psi = Q_\psi \tag{6}$$

where the momenta p_θ, p_ϕ, and p_ψ are defined in Appendix B, in terms of the velocities and displacements, and the nonconservative generalized forces Q_θ, Q_ϕ, and Q_ψ are derived from the torque and damping force in the next section.

GENERALIZED FORCES

Since the generalized coordinates are angles, the generalized forces have the units of torque (in - lb). They are obtained from the virtual work of

the driving or shaft torque T_s, the disk load torque T_L, and the damping force F_d, as follows:

The total virtual work is

$$\delta W = \delta W_s + \delta W_L + \delta W_d \tag{7}$$

The virtual work of the shaft torque T_s is

$$\delta W_s = T_s\left[\delta\phi + \delta\psi\right]. \tag{8}$$

The virtual work of the disk load torque T_L is

$$\delta W_L = T_L\left[\cos\theta\delta\phi + \delta\psi\right]. \tag{9}$$

In general, T_L is proportional to some power n of the disk speed ω_z.

Two cases are considered here: n = 1 (viscous), and n = 2 (aerodynamic).

For n = 1,

$$T_L = -C_L\omega_z = -C_L\left[\dot{\phi}\cos\theta + \dot{\psi}\right], \tag{10}$$

and for n = 2,

$$T_L = -\frac{\omega_z}{|\omega_z|}\,\bar{C}_L\left[\dot{\phi}\cos\theta + \dot{\psi}\right]^2, \tag{11}$$

where C_L and $\bar{C}_L$ are the disk load coefficients for viscous torque and aerodynamic torque, respectively.

The virtual work of the damping force $\vec{F}_d$ is

$$\delta W_d = -F_{d_\theta}\ell\delta\theta - F_{d_\phi}\ell\sin\theta\delta\phi\ , \tag{12}$$

where $\vec{F}_{d_\theta}$ and $\vec{F}_{d_\phi}$ are the radial and tangential components of $\vec{F}_d$, respectively.

If $\vec{F}_d$ is predominantly due to the drag of the disk in the working fluid, it will be proportional to some power n' = n for each of the two cases above (viscous and aerodynamic drag, respectively).

For n = 1,

$$\overrightarrow{F_d} = -C_d\sqrt{(\ell\sin\theta\dot{\phi})^2 + (\ell\dot{\theta})^2}\ , \tag{13}$$

$$F_{d_\theta} = -C_d\ell\dot{\theta}\ , \tag{14}$$

$$F_{d_\theta} = -C_d(\ell\sin\theta)\dot{\phi}\ , \tag{15}$$

where C_d is the viscous damping coefficient.

For n = 2,

$$\overrightarrow{F_d} = -\bar{C}_d\left[(\ell\sin\theta\dot{\phi})^2 + (\ell\dot{\theta})^2\right], \tag{16}$$

$$F_{d_\theta} = -\bar{C}_d\ell\dot{\theta}\sqrt{(\ell\sin\theta\dot{\phi})^2 + (\ell\dot{\theta})^2}\ , \tag{17}$$

$$F_{d_\phi} = -C_d\ell\sin\theta\dot{\phi}\sqrt{(\ell\sin\theta\dot{\phi})^2 + (\ell\dot{\theta})^2}\ , \tag{18}$$

where $\bar{C}_d$ is the aerodynamic damping coefficient.

In all cases the direction of $\vec{F}_d$ is assumed to be tangent to the path of the disk center C, opposing the motion.

For the viscous case, substitution of (14) and (15) into (12), (10) into (9), and (8), (9) and (12) into (7) yields the total virtual work, which can be factored into the form

$$\delta W = Q_\theta\delta\theta + Q_\phi\delta\phi + Q_\psi\delta\psi. \tag{19}$$

Substitution of equations (1), (2), and (3) into the expressions for Q_θ, Q_ϕ, and Q_ψ gives

$$Q_\theta = -C_d\frac{\ell^2}{I_{x'}}p_\theta\ , \tag{20}$$

$$Q_\phi = T_s - \frac{C_d\ell^2}{I_{x'}}p_\phi + \left[\frac{C_d\ell^2}{I_{x'}} - \frac{C_L}{I_z}\right]\cos\theta p_\psi\ , \tag{21}$$

$$Q_\psi = T_s - \frac{C_L}{I_z}p_\psi \tag{22}$$

For the aerodynamic case, a similar procedure using (11), (17) and (18) gives

$$Q_\theta = -\bar{C}_d\ell^3\frac{p_\theta}{I_{x'}^2\sin\theta}\sqrt{\left[p_\phi - \cos\theta p_\psi\right]^2 + \sin^2\theta p_\theta^2}\ , \tag{23}$$

$$Q_\phi = T_s - \frac{p_\psi}{|p_\psi|}\frac{\bar{C}_L\cos\theta}{I_z^2}p_\psi^2 - \bar{C}_d\ell^3\frac{\left[p_\phi - \cos\theta p_\psi\right]}{I_{x'}^2\sin\theta}\sqrt{\left[p_\phi - \cos\theta p_\psi\right]^2 + \sin^2\theta p_\theta^2} \tag{24}$$

$$Q_\psi = T_s - \frac{p_\psi}{|p_\psi|}\frac{C_L}{I_z^2}p_\psi^2 \tag{25}$$

THE TORQUEWHIRL SOLUTIONS

The differential equations of motion for the rotor of Fig. 1 are given by (1) through (6), with Q_θ, Q_ϕ, and Q_ψ substituted from (20), (21) and (22) for the case with viscous load torque and damping, or from (23), (24), and (25) for the case with aerodynamic load torque and damping.

For both cases, an exact solution to the equations of motion is found which describes nonsynchronous whirling at constant amplitude, as follows:

Viscous case

The ratio of whirling speed to shaft speed is defined as

$$f = \frac{\dot{\phi}}{\omega_s} \tag{26}$$

then

$$p_\theta = \theta \ ,$$

$$p_\phi = I_x' f \omega_s \sin^2\overset{*}{\theta} + I_z\left[1 - f(1 - \cos\overset{*}{\theta})\right]\omega_s \cos\overset{*}{\theta} \ ,$$

$$p_\psi = I_z\left[1 - f(1 - \cos\overset{*}{\theta})\right]\omega_s \ , \tag{27}$$

$$\dot{p}_\theta = 0 \ ,$$

$$\dot{p}_\phi = 0 \ ,$$

$$\dot{p}_\psi = 0 \ ,$$

is a solution, where $\overset{*}{\theta}$ is the value of θ which satisfies the following equation:

$$\frac{R_c(1 - \cos\theta)}{R_c(1 - \cos\theta)^2 + \sin^2\theta} = \frac{I_2 \pm \sqrt{I_2^2 + \frac{4}{\omega_s^2}(I_1\cos\theta + I_2)(\mu_g^2 + \mu_K^2 \frac{\theta}{\sin\theta})}}{2(I_1\cos\theta + I_2)} \ , \tag{28}$$

and the whirling speed ratio f is then given by the right hand side of (28). That is,

$$f = \frac{I_2 + \sqrt{I_2^2 + \frac{4}{\omega_s^2}(I_1\cos\overset{*}{\theta} + I_2)(\mu_g^2 + \mu_K^2 \frac{\overset{*}{\theta}}{\sin\overset{*}{\theta}})}}{2(I_1\cos\overset{*}{\theta} + I_2)} \tag{29}$$

where

$$I_1 = \frac{I_x' - I_z}{I_x'} \ , \quad I_2 = \frac{I_z}{I_x'} \ ,$$

$$\mu_g^2 = \frac{Mg\ell}{I_x'} \ , \quad \mu_K^2 = \frac{K_\theta}{I_x'} \ ,$$

and

$$R_c = \frac{C_L}{C_d \ell^2} \ .$$

AERODYNAMIC CASE

The equations of motion for this case are also satisfied by (27), with the whirling speed ratio f given by (29), where $\overset{*}{\theta}$ is now the value of θ which satisfies

$$\frac{\pm\sqrt{(1 - \cos\theta)\sin^3\theta \bar{R}_c} - (1 - \cos\theta)^2 \bar{R}_c}{\sin^3\theta - (1 - \cos\theta)^3 \bar{R}_c}$$

$$= \frac{I_2 \pm \sqrt{I_2^2 + \frac{4}{\omega_s^2}(I_1\cos\theta + I_2)(\mu_g^2 + \mu_K^2 \frac{\theta}{\sin\theta})}}{2(I_1\cos\theta + I_2)} \tag{30}$$

where

$$\bar{R}_c = \frac{\bar{C}_L}{\bar{C}_d \ell^3} \ , \text{ and}$$

I_1, I_2, μ_g, μ_K are defined the same as for the viscous case.

For both cases, the method of numerical solution is as follows :

1. Assume a value of $\overset{*}{\theta}$ and use it to calculate f from (29).
2. Calculate R_c or $\bar{R}_c$ from (28) or (30) respectively.
3. Calculate the shaft torque and/or damping from R_c or $\bar{R}_c$.

Step 2 is simplified for both cases by substituting f for the right hand side of (28) or (30), then solving (28) explicitly for R_c, or (30) for $\bar{R}_c$. The resulting expressions for R_c and $\bar{R}_c$ are :

$$R_c = \frac{f\sin^2\overset{*}{\theta}}{(1 - \cos\overset{*}{\theta})\left[1 - f(1 - \cos\overset{*}{\theta})\right]} \ , \tag{31}$$

$$\bar{R}_c = \frac{f^2\sin^3\overset{*}{\theta}}{(1 - \cos\overset{*}{\theta})\left[1 - f(1 - \cos\overset{*}{\theta})\right]^2} \ . \tag{32}$$

NUMERICAL RESULTS AND DISCUSSION

The equations of the preceding section were programmed for digital computation on the IBM-360-MOD65 computer at the University of Florida. In general, small angle assumptions were not made, even though the angles are small, since the precise magnitude of θ is of prime interest and since some of the computations are strong functions[2] of θ. Results are shown in Figs. 2 through 7.

Fig. 2 shows how the whirling speed ratio f varies with shaft speed. For any given rotor geometry, f becomes rather constant at high speeds where the gyroscopic forces are strong. This causes the actual whirling frequency to become higher than the critical speed at high shaft speeds. This effect is independent of the type of loading or damping.

Fig. 3 shows how the ratio of load torque to damping (R_c or $\bar{R}_c$) varies with whirling speed ratio

2. Wherever this is not the case, it is so indicated on the curves.

f, for both types of loading. The value of R_c or R_c read from the curves should be interpreted as the ratio of load torque to damping required to produce torquewhirl at a given frequency.

Fig. 4 shows how the whirling amplitude θ increases with the ratio of load torque to damping. For a given rotor at a given speed, the appropiate value of f can be taken from Fig. 2. Note that Figs. 3 and 4 are independent of the mass or stiffness properties of the rotor (except insofar as they determine the value of f).

PROTOTYPE MACHINE

To illustrate some specific results which could be observed in a compressor or pump, a prototype machine is defined below. The chosen design and performance parameters are believed to be representative of some modern high speed machines (although the present model restricts the prototype to a single disk, or stage). These are:

Maximun horsepower - 2500 at 8000 RPM
Maximun speed - 8000 RPM
Critical speed - about 3200 RPM
Disk weight - 25 pounds
Disk radius - 7.5 inches
Effective shaft stiffness - 10^5 in-lb/rad

The damping and shaft lenght are treated as design variables, since they each could be used to suppress torquewhirl without compromising machine performance.

Figs. 5, 6, and 7 show representative results for this particular machine.

Fig. 5 gives the load horsepower required to produce various amplitudes of torquewhirl as a function of shaft speed. The corresponding whirling frequencies are also given. For example, at 8000 RPM, a load of about 1100 horsepower is required to produce a whirling amplitude of 10 mils at a frequency of 0.71 times shaft speed. This is for ℓ = 5.5 inches and 5% equivalent damping.

Since damping is ussually computed on a linear basis, it is presented this way in Figs. 5 and 6. This makes the nonlinear damping coefficient $\bar{C}_d$ amplitude dependent, so the results are normalized to an amplitude of 47 mils. For q% damping, the coefficient is then given by

$$\bar{C}_d = \frac{C_d}{(.047)f\omega_s} \quad , \tag{33}$$

where

$$C_d = \frac{q}{100}\left[2M\sqrt{\omega_s^2 + \omega_g^2}\right] . \tag{34}$$

Fig. 6 shows that the load horsepower required to produce a given amplitude of torquewhirl can be increased by increasing the damping. However, the amount of added damping required to produce significant reductions may become impractically large. For example, extrapolation of the curves shows that the damping would need to be approximately doubled to reduce the amplitude from 20 mils to 10 mils, for a load of 2000 horsepower.

The most effective way of avoiding torquewhirl may be through optimization of the shaft length ℓ, as suggested by Fig. 7. The optimun shaft lenght is that which maximizes the required horsepower. A tradeoff must be made with synchronous response to unbalance, however, since the curve shows that optimun ℓ means operation at or near the critical speed (f = 1).

OTHER MACHINES

It is interesting to speculate as to how the torquewhirl characteristics demonstrated by this simple model might be manifested in machines of greater complexity. For example, a disk mounted between two bearings on a flexible shaft (not at mid-span) can execute a coning motion with a potential for torquewhirl. Multiple disks on a flexible shaft are an extension of this case, in which torquewhirl could occur at a multiplicity of frequencies, each with a different required load torque and horsepower. The coning angle of each disk would be determined by the mode shape associated with the particular frequency.

Although the results were not presented graphically, it was found that increasing the shaft stiffness in the model of Fig. 1 tends to increase the load torque or horsepower requiered to produce a given amplitude of torquewhirl, when the whirling speed ratio is less than unity.

If this analysis qualitatively predicts the characteristics of more complex machines, it should be expected that nonsynchronous whirl produced by high load torque can be effectively suppressed by stiffening flexible shafts to reduce the coning angles and move the whirling speed ratio closer to 1.0 (see Fig. 7). Where this is not practical, it may be found helpful to selectiveley modify the shaft stiffness at specific lacations to reduce the coning angles of those disks with the largest load torque and/or misalignment in the mode shape at the troublesome frequency. Clearly, more work needs to be done to verify and expand on these concepts for flexible-shaft machines.

All of the solutions described here are for forward whirl in negativework machines (i.e. compressors, pumps, etc.) in which the disk is driven by the shaft to do work on the fluid. No solutions were found for backward whirl of such machines.

For positive-work machines (i.e. turbines), backward whirl was found to be a solution with driving torque on the disk, but the equations used here for the torque-speed relationship probably do not represent a realistic model for turbines, so this solution is not given.

COEFFICIENTS FOR LINEARIZED STABILITY ANALYSIS

The equations presented above are exact solutions to the differential equations of motion. They represent the limit cycles of subsynchronous whirling, and therefore allow the computation of whirl amplitudes. Such solutions cannot be practically obtained for more complex models, so a linearized stability analysis is used to compute the whirl frequencies, threshold speeds of instability, and the logarithmic decrements (i.e. the eigenvalues).

Lund [11] has extended the Myklestad - Prohl transfer matrix method to rotor-bearing systems wich include damping and destabilizing cross - coupled stiffness and damping coefficients. Whereas the Myklestad-Prohl method yields only the imaginary part of the eigenvalues (i.e. the natural frequencies), the Lund method yields complex eigenvalues (i.e. both the natural frequencies and the logarithmic decrement, wich is a stability predictor).

For the rigid-shaft, flexible joint, torquewhirl model in Figure 1, the disk rotation and translation coordinates are not independent (i. e. they are related by a kinematic constraint). The constraint equations are $R = \ell\theta$ in polar coordinates or $x^2 + y^2 = (\ell \sin\theta)^2$ in inertial coordinates.

Since the differential equations and generalized forces are written in terms of Euler angles ϕ, θ, and ψ, a coordinate transformations is required to derive the stiffness and damping coefficients, as follows :

First, the generalized torque Q_ϕ can be expressed as a tangential for

$$F_\phi = Q_\phi / R,$$

and the generalized moment Q_θ can be radial force

$$F_R = Q_\theta / \ell \cos\theta$$

It is Q_ϕ (or F_ϕ) which contains the destabilizing torquewnirl forces.
The transformation to x and y is

$$F_x = F_R \cos\phi - F_\phi \sin\phi$$
$$F_y = F_R \sin\phi + F_\phi \cos\phi \qquad \ldots(39)$$

where

$$\sin\phi = \frac{y}{(x^2 + y^2)^{1/2}}$$

$$\cos\phi = \frac{x}{(x^2 + y^2)^{1/2}} \qquad \ldots(40)$$

For the aerodynamic case, the generalized torque Q_ϕ is

$$Q_\phi = T_s - \bar{C}_L (\dot{\psi} + \dot{\phi}\cos\theta)^2 \cos\theta - \bar{C}_d (\ell^3 \sin^3\theta)\, \dot{\phi}^2 , \qquad \ldots(41)$$

where

T_s = shaft torque

$\bar{C}_L$ = disk load coefficient

$\bar{C}_d$ = nonlinear damping coefficient

Currently the greatest limitation of Lund's method (as with all other stability analyses) is the lack of accurate information about the types of destabilizing excitations which exist in real machines and which therefore are to be used as imput to the computer program. Torquewhirl has here been identified as one of these excitations. To put the torquewhirl forces into a Lund stability analyses, they must be formulated in terms of stiffness and damping coefficients.

The coordinates used in Lund's analysis are shown in Figure 8. In general, the stiffness and damping coefficients are the matrices which define the forces and moments on each disk in the x and y directions.

For example, the force on a disk in the x direction, due to disk displacement and velocity, is

$$F_x = -K_{xx} X - K_{xy} Y - C_{xx} \dot{X} - C_{xy} \dot{Y} - K_{x\alpha}\alpha - K_{x\beta}\beta - C_{x\alpha}\dot{\alpha} - C_{x\beta}\dot{\beta} \qquad (35)$$

and the matrix equation for the forces in all directions (on a single disk) is

$$\begin{Bmatrix} F_x \\ F_y \\ F_\alpha \\ F_\beta \end{Bmatrix} = - \begin{bmatrix} K_{xx} & K_{xy} & K_{x\alpha} & K_{x\beta} \\ K_{yx} & K_{yy} & K_{y\alpha} & K_{y\beta} \\ K_{\alpha x} & K_{\alpha y} & K_{\alpha\alpha} & K_{\alpha\beta} \\ K_{\beta x} & K_{\beta y} & K_{\beta\alpha} & K_{\beta\beta} \end{bmatrix} \begin{Bmatrix} x \\ y \\ \alpha \\ \beta \end{Bmatrix} - \begin{bmatrix} C_{xx} & C_{xy} & C_{x\alpha} & C_{x\beta} \\ C_{yx} & C_{yy} & C_{y\alpha} & C_{y\beta} \\ C_{\alpha x} & C_{\alpha y} & C_{\alpha\alpha} & C_{\alpha\beta} \\ C_{\beta x} & C_{\beta y} & C_{\beta\alpha} & C_{\beta\beta} \end{bmatrix} \begin{Bmatrix} \dot{X} \\ \dot{Y} \\ \dot{\alpha} \\ \dot{\beta} \end{Bmatrix} ,$$

where F_α and F_β are actually moments on the disk.

It can be seen that there are a total of thirty two stiffness and damping coefficients defining the forces and moments on each disk. The off-diagonal elements are called the cross-coupled coefficients.

The shaft speed ω_s is

$$\omega_s = \dot{\psi} + \dot{\phi}. \qquad (42)$$

The shaft torque equals the disk load torque so that

$$T_s = \bar{C}_L (\dot{\psi} + \dot{\phi}\cos\theta)^2 \qquad (43)$$

Therefore the generalized torque Q_ϕ can be expressed as

$$Q_\phi = T_s [1 - \cos\theta] - \bar{C}_d (\ell^3 \sin^3\theta)\, \dot{\phi}^2 . \qquad (44)$$

The destabilizing part of Q_ϕ is the first term from the expression just above. The equivalent tangential force F_ϕ is

$$F_\phi = \frac{Q_\phi}{R} = \frac{T_s(1 - \cos\theta)}{R} \tag{45}$$

The required relationships between R, θ, and α, β, and x, y are

$$R = (x^2 + y^2)^{\frac{1}{2}}$$

$$x = \alpha\ell$$

$$y = \beta\ell \tag{46}$$

$$\text{and } \theta = (\alpha^2 + \beta^2)^{\frac{1}{2}}$$

Therefore, in terms of x and y, we can write

$$F_\phi = \frac{T_s\left[1 - \cos\frac{(x^2 + y^2)^{\frac{1}{2}}}{\ell}\right]}{(x^2 + y^2)^{\frac{1}{2}}} \tag{47}$$

Keeping only the first two terms of the cosine series yields

$$F_\phi = \frac{T_s}{2\ell^2}(x^2 + y^2)^{\frac{1}{2}} \tag{48}$$

or

$$F_x = -F_\phi \sin\phi = -\frac{T_s}{2\ell^2} y,$$

$$F_y = F_\phi \cos\phi = \frac{T_s}{2\ell^2} x \tag{49}$$

By inspection, it can be seen that the cross-coupled stiffness are

$$K_{xy} = \frac{T_s}{2\ell^2}$$

$$K_{yx} = -\frac{T_s}{2\ell^2} \tag{50}$$

It is interesting to note that K_{xy} and K_{yx} have the same form as Alford's coefficients for the effect of tip clearance assymmetry in axial flow turbomachinery [12].

As a crude approximation, the above coefficients (K_{xy}, K_{yx}) could be used for a flexible-shaft model by taking ℓ as the axial distance from the disk plane to a virtual pivot point, as determined by the mode shape.

When the rotor flexibility is distributed along the shaft, there is no constraint between x, y and α, β. Therefore the virtual work of the destabilizing torque must be written in terms of x, y, α, and β. This requires that the virtual displacement $\delta\phi$ be written in terms of δx, δy, $\delta\alpha$, and $\delta\beta$.

Since the rotations of a disk are independent of the translations, it can be seen that δx and δy will not appear in $\delta\phi$. This leaves only the virtual angular displacements $\delta\alpha$ and $\delta\beta$ to be considered. A kinematical relationship between ϕ,α, and β is thus required. Research is now in progress at Texas A&M University along these lines.

CONCLUSIONS

From the analysis and discussion given above, the following conclusions are drawn:

1. Exact solutions to the complete nonlinear equations of motion for a rotor with high load torque and a coning disk show that constant torque can produce nonsynchronous whirling with an amplitude which depends mainly on the ratio of torque to damping and the whirling speed ratio. All other things being equal, the whirling amplitude is directly dependent on the magnitude of the load torque. The solutions given thus constitute a mathematically proven theory which can explain a number of nonsynchronous whirling failures in compressors and pumps under load.

2. No-load tests of compressors, pumps, and other negative-work machines are not sufficient to demonstrate smooth and safe machine operation. A machine can pass a no-load test to full speed with no whirling problems and yet whirl violently when an attempt is made to bring it up to load.

3. Torquewhirl can be suppressed in a given machine by increasing the damping, optimizing the shaft length, and/or stiffening the shaft. The amount of damping required to reduce the whirling amplitude to an acceptable level may not always be practically achievable. Since the optimun shaft to maximize the horsepower required for torquewhirl is the one which produces a whirling speed ratio of unity (operation at the critical speed), a tradeoff must be made with synchronous response to unbalance.

4. Cross-coupled stiffness coefficients for linearized stability analysis were derived for the special case of Figure 1 (rigid shaft with flexible joint). Additional work is now in progress to derive cross-coupled angular stiffness coefficients for a rotor model with a flexible shaft.

ACKNOWLEDGEMENTS

Major portions of the research presented here were supported by grants from the U.S. Army Research Office and the National Science Foundation (U.S.A.). The part giving exact solutions was first published in The Transactions of the American Society for Mechanical Engineers: Journal of Engineering for Power, April, 1978.

REFERENCES

1) Wachel, J.C.: *"Nonsynchronous Instability of Centrifugal Compressors"*. ASME Paper No. 75-Pet -22, Petroleum Mechanical Engeneering Conference, Tulsa, Oklahoma September 21-25, 1975.

2) Smith, D.M.: Journal Bearings in Turbomachinery, Chapman and Hall Ltd., London, 1969, page 127.

3) Alford, J.S.: *"Protecting Turbomachinery From Self-Excited Rotor Whirl"*. ASME Journal of Engineering for Power, October, 1965, pp. 333-344.

4) Dimentberg, F.M.: Flexural Vibrations of Rotating Shafts, Butterworths, London, 1961, page 17.

5) Gunter, E.J., Jr.: *"Dynamic Stability of Rotor-Bearing Systems"*. NASA SP-113, 1966, pp. 25-42.

6) Eshleman, R.L. and Eubanks, R.A.: *"Effects of Axial Torque on Rotor Response: An Experimental Investigation"*. ASME Paper No. 70-WA/DE-14,ASME Winter Annual Meeting, November 29-December 3, 1970, New York.

7) Bousso, D.: *"A Stability Criterion for Rotating Shafts"*. Israel Journal of Technology, Vol. 10, No. 6, pp. 409-423.

8) Goldstein, H.: Classical Mechanics, Addison - Wesley Publishing Co., Inc., Reading, Mass., 1950, page 107.

9) Vance, J.M. and Sitchin, A.: *"Derivation of First-Order Difference Equations for Dynamical Systems by Direct Application of Hamilton's Principle"*. ASME Journal of Applied Mechanics, June 1970, pp. 276-278.

10) Vance, J.M. and Sitchin, A.: *"Numerical Solution of Dynamical Systems By Direct Application of Hamilton's Principle"*. International Journal For Numerical Methods In Engineering, Vol. 4, pp. 207-216.

11) Lund, J.W.: *"Stability and Damped Critical Speeds of a Flexible Rotor in Fluid-Film Bearings"*. ASME Journal of Engineering for Industry, May 1974, pp. 509-517.

12) Alford, J.S.: *"Protecting Turbomachinery From Self-Excited Rotor Whirl"*. ASME Journal of Engineering for Power, October 1965, pp. 333-334.

APPENDIX A

In terms of the angular velocities about body-fixed principal axes x' y' z through 0' (see Fig. 1), the kinetic energy of the rotor is

$$T = \frac{1}{2} I_{x'} \omega_{x'}^2 + \frac{1}{2} I_{y'} \omega_{y'}^2 + \frac{1}{2} I_z \omega_z^2 \qquad (A\text{-}1)$$

The kinematic relationships required to express T in terms of the generalized coordinates are:

$$\begin{aligned} \omega_{x'} &= \dot{\theta}\cos\psi + \dot{\phi}\sin\psi\sin\theta \\ \omega_{y'} &= -\dot{\theta}\sin\psi + \dot{\phi}\cos\psi\sin\theta \\ \omega_z &= \dot{\phi}\cos\theta + \dot{\psi} \end{aligned} \qquad (A\text{-}2)$$

The potential energy is

$$V = \frac{1}{2} K_\theta \theta^2 + Mg\ell(1 - \cos\theta) \qquad (A\text{-}3)$$

Substitution of (A-2) into (A-1), with $I_{x'}=I_{y'}$, gives the Lagrangian as

$$\begin{aligned} L = T - V = {} & \frac{1}{2}\left[I_x + M\ell^2\right](\dot{\theta}^2 + \dot{\phi}^2 \sin^2\theta) \\ & + \frac{1}{2} I_z(\dot{\psi}^2 + \dot{\phi}^2\cos^2\theta + 2\dot{\phi}\dot{\psi}\cos\theta) \\ & - \frac{1}{2} K_\theta \theta^2 - Mg\ell(1 - \cos\theta). \end{aligned} \qquad (A\text{-}4)$$

APPENDIX B

Refences 9 and 10 show how first-order differential equations of motion can be easily derived in mixed form (including both momenta and velocities) from the Lagrangian. The canonical form can be obtained by substituting expressions in terms of the momenta for the velocities, and without the necessity to derive the Hamiltonian. The advantages of the resulting first-order equations are that the solution can be obtained with only one integration, and the form of the equations is inmediately suitable for stability analysis after linearization (not done here). Furthermore, the need to take the time derivatives specified by Lagrange's equation is eliminated. If the reader prefers to work with Lagrange's equations, these can be derived by substituting the momenta into equations (4), (5), and (6), and taking the indicated derivatives. The momenta are:

$$p_\theta = \frac{\partial L}{\partial \dot{\theta}} = I_{x'}\dot{\theta}, \qquad (B\text{-}1)$$

$$p_\phi = \frac{\partial L}{\partial \dot{\phi}} = I_{x'}\dot{\phi}\sin^2\theta + I_z(\dot{\psi} + \dot{\phi}\cos\theta)\cos\theta, \qquad (B\text{-}2)$$

$$p_\psi = \frac{\partial L}{\partial \dot{\psi}} = I_z(\dot{\psi} + \dot{\phi}\cos\theta), \qquad (B\text{-}3)$$

where L is derived in Appendix A.

Recibido el 1º de marzo de 1983

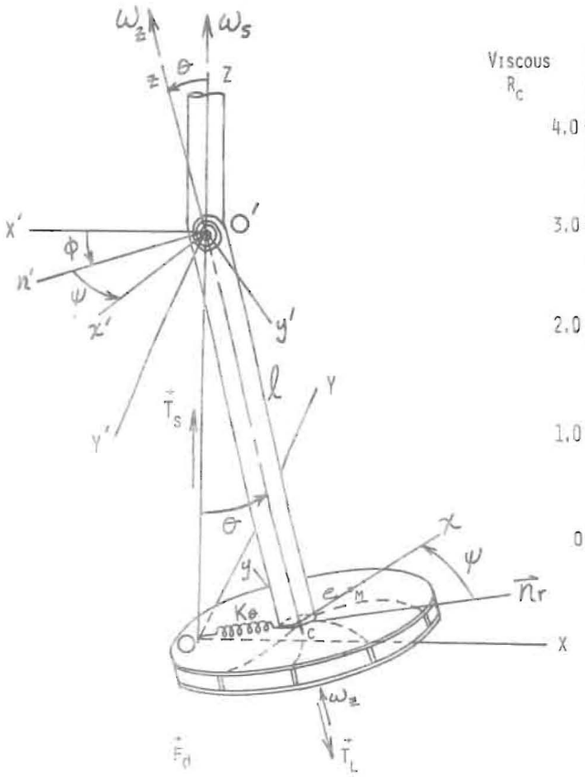

FIG. 1: "TORQUEWHIRL" MODEL

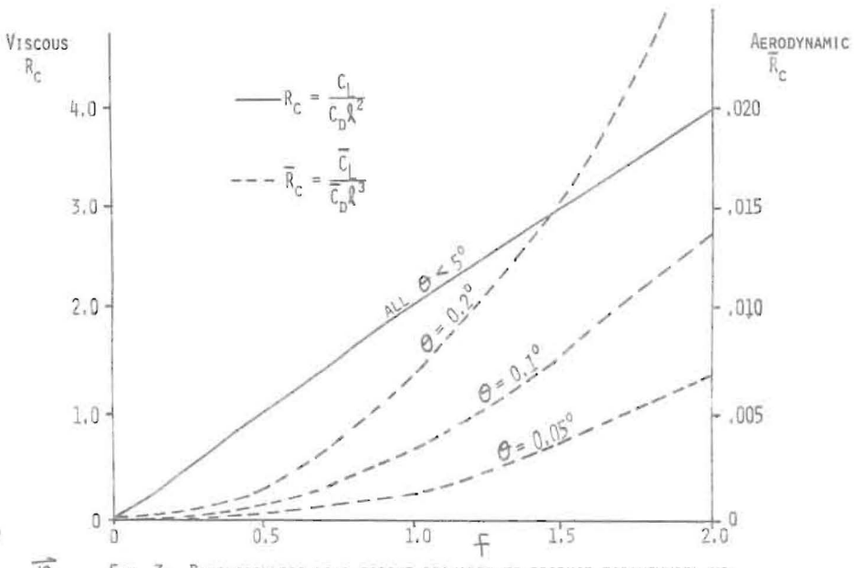

FIG. 3: DIMENSIONLESS LOAD TORQUE REQUIRED TO PRODUCE TORQUEWHIRL VS. WHIRLING SPEED RATIO, VISCOUS AND AERODYNAMIC CASES

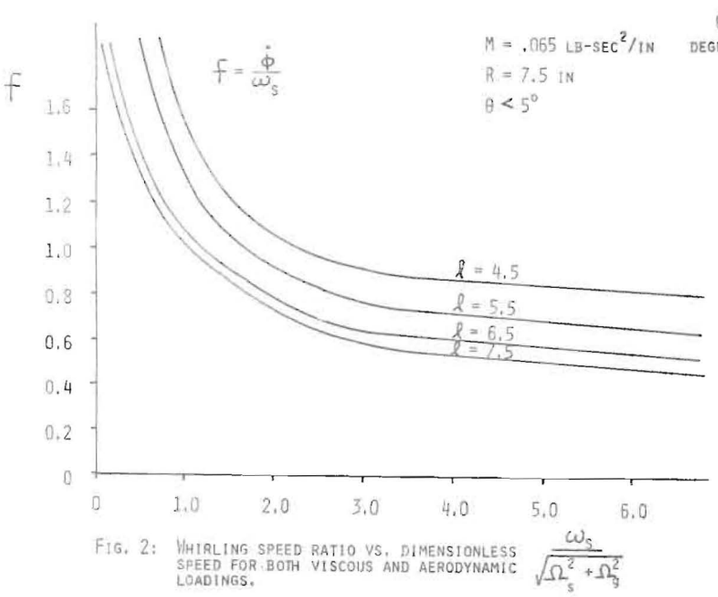

FIG. 2: WHIRLING SPEED RATIO VS. DIMENSIONLESS SPEED FOR BOTH VISCOUS AND AERODYNAMIC LOADINGS.

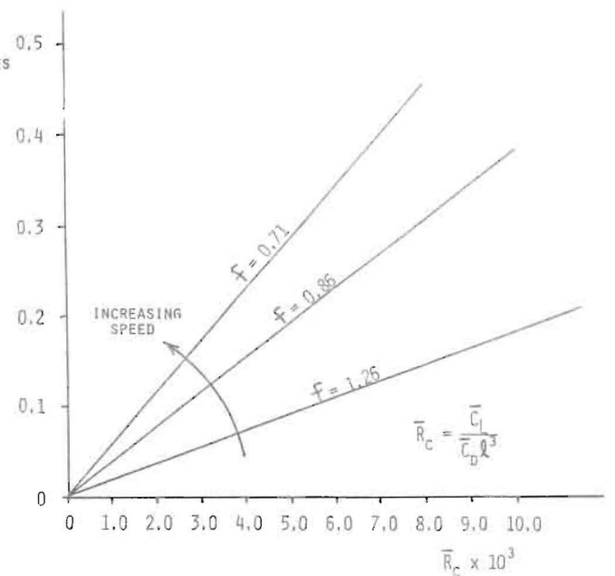

FIG. 4: WHIRLING AMPLITUDE VS. DIMENSIONLESS LOAD TORQUE, AERODYNAMIC CASE.

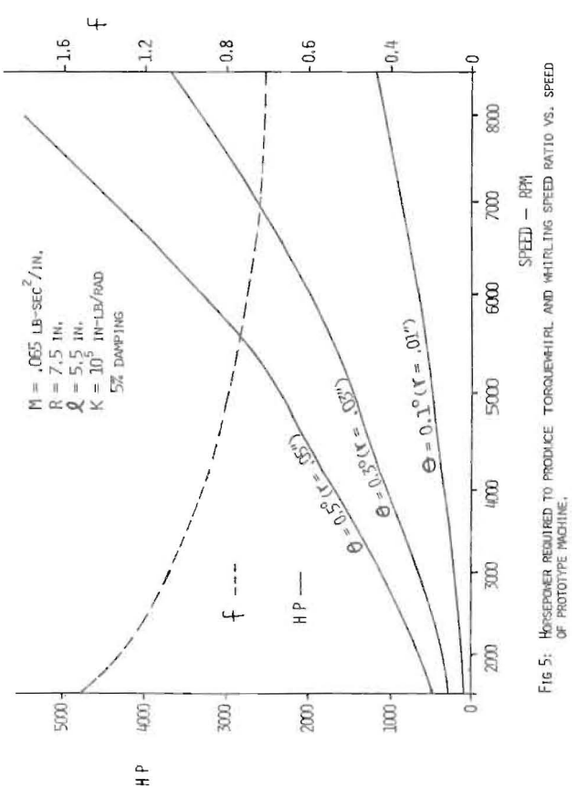

FIG 5: HORSEPOWER REQUIRED TO PRODUCE TORQUEWHIRL AND WHIRLING SPEED RATIO VS. SPEED OF PROTOTYPE MACHINE.

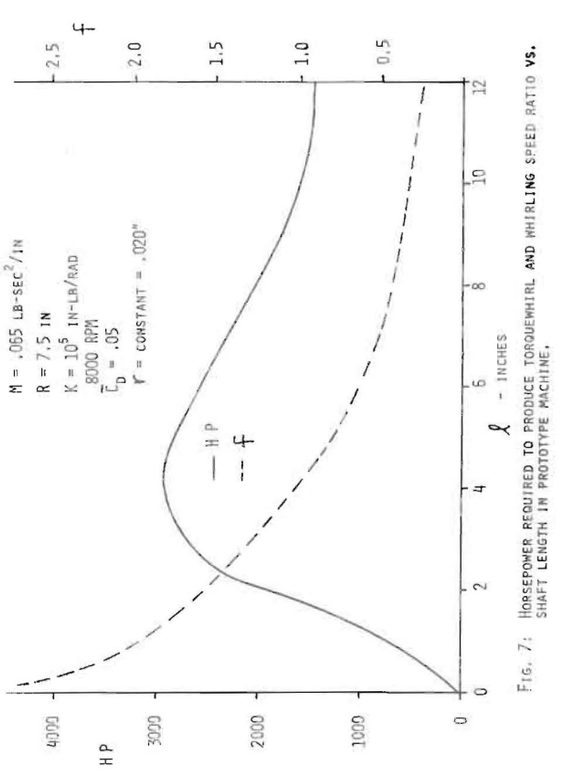

FIG. 7: HORSEPOWER REQUIRED TO PRODUCE TORQUEWHIRL AND WHIRLING SPEED RATIO VS. SHAFT LENGTH IN PROTOTYPE MACHINE.

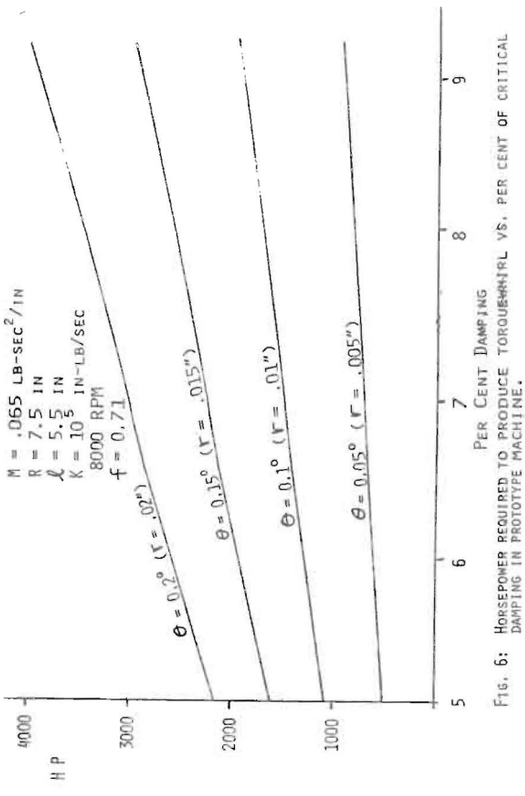

FIG. 6: HORSEPOWER REQUIRED TO PRODUCE TORQUEWHIRL VS. PER CENT OF CRITICAL DAMPING IN PROTOTYPE MACHINE.

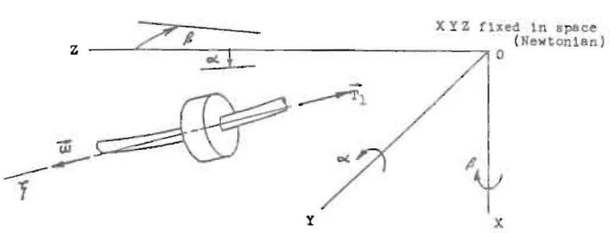

Fig. 8: COORDINATES FOR LINEARIZED STABILITY ANALYSIS